Journal of Molecular Spectroscopy 262 (2010) 69–74

Contents lists available at ScienceDirect

Journal of Molecular Spectroscopy

journal homepage: www.elsevier.com/locate/jms

Deperturbation study of the $d^3\Pi_g$, $v' = 4$ state of C_2 by applying degenerate and two-color resonant four-wave mixing

P. Bornhauser, G. Knopp, T. Gerber, P.P. Radi *

Department General Energy, Paul Scherrer Institute, CH-5232 Villigen, Switzerland

ARTICLE INFO

Article history:
Received 27 April 2010
In revised form 19 May 2010
Available online 2 June 2010

Keywords:
C_2
Deperturbation
Four-wave mixing

ABSTRACT

The potential of four-wave mixing spectroscopy in combination with a discharge slit-jet source is explored by performing an analysis of the perturbations occurring between vibronic levels of the $d^3\Pi_g$, $v' = 4$ and $b^3\Sigma_g^-$, $v' = 16$ states of C_2. Unambiguous assignments of perturbed transitions are achieved by intermediate level labeling in the $a^3\Pi_u$ state of the Swan system and results in the re-assignment of several line positions found in the literature. Furthermore, extra transitions are observed and assigned in a straightforward manner that originate from the perturbing $b^3\Sigma_g^-$, $v' = 16$ electronic state. Significantly perturbed rotational transitions in the (4,3) band of the Swan system are reported for the first time. A least-squares fit to 35 perturbed and perturbing transitions yields the vibronic origin, rotational and spin-spin coupling constant of the $b^3\Sigma_g^-$, $v' = 16$ state as well as the spin-orbit and L-uncoupling parameters for the interaction between the $d^3\Pi_g$, $v' = 4$ and $b^3\Sigma_g^-$, $v' = 16$ states.

1. Introduction

The Swan band emission of C_2 in the visible spectral range between 400–600 nm is readily observed in all carbon-containing flames. The strong $d^3\Pi_g - a^3\Pi_u$ electronic system has been used to detect this minor species in combustion processes by applying numerous experimental techniques such as laser-induced fluorescence (LIF) [1–3], chemiluminescence [1], degenerate four-wave mixing (DFWM) [4,5], cavity ring-down (CRD) [2,6,7] and intracavity laser absorption spectroscopy (ICL) [8]. In addition, a recent experiment reports on the application of polarization spectroscopy of C_2 to visualize soot formation [9] and LIF for soot volume fraction measurements [10]. C_2 Swan emission is observed to study thermal and dynamical properties of plumes produced by laser ablation of graphite targets [11–14]. In addition, it has been shown that C_2 Swan band emission is often present when intense laser fields irradiate carbon-containing compounds in the visible or ultraviolet spectral range [15,16]. In the interstellar medium, the dicarbon molecules have been detected in diffuse and translucent clouds, in the cirumstellar shell of carbon stars and in comets as well and they play an important role in the formation of hydrogen-deficient carbon molecules and the formation of cyclic molecules [17,18].

Quantitative interpretation of spectra requires a detailed understanding of the signal generation process and precise molecular constants for the computation of the complex molecular spectra of C_2. In particular for the application of non-linear optical methods such as degenerate and two-color resonant four-wave mixing, the computation of the correct spectral intensities is critically dependent on the relative positions of unresolved components because a coherent addition of overlapping transitions is required [19]. Furthermore, accurate molecular constants of the carbon dimer are needed in situations, where spectral features consist of multiple unresolved components [8,11]. In fact, this study has been motivated partially by our recent experiments on radicals in a free-jet emerging from discharged hydrocarbon/argon mixtures. The spectra of these molecules are often superimposed with strong Swan band transitions. Obviously, an unambiguous assignment of these lines is mandatory to disentangle the spectral observations.

However, the most recent molecular constants [20] are not sufficiently complete to model all features of the $d^3\Pi_g - a^3\Pi_u$ system because of local perturbations in many vibrational levels. Despite the fact that the $d^3\Pi_g - a^3\Pi_u$ system of C_2 has been studied for over 200 years, a complete rotational analysis has not been achieved. Difficulties arise mainly due to the interaction of the Swan levels with several neighboring electronic states within the triplet and the singlet manifold. In fact, perturbations in the $d^3\Pi_g - a^3\Pi_u$ electronic system have already been discussed in the early 1960's. Callomon and Gilby [21] reported that perturbations in the $v' = 0, 1$ and 2 level of the $d^3\Pi_g$ electronic state are due to interactions with the vibronic levels $v' = 11-16$ of the $b^3\Sigma_g^-$ state. Another perturbation was assigned to an interaction with the $B^1\Delta_g$, a state that had been discovered only later by Douay et al. [22]. Phillips [23] extended the work of Callomon and Gilby to the $v' = 3, 4, 5$ levels. Observed perturbations were rationalized by

* Corresponding author. Fax: +41 563102199.
E-mail address: peter.radi@psi.ch (P.P. Radi).

0022-2852/$ - see front matter © 2010 Elsevier Inc. All rights reserved.
doi:10.1016/j.jms.2010.05.008

taking into account the $b^3\Sigma_g^-$ and, in addition, the $X^1\Sigma_g^+$ ground state, but certain observations were left unexplained.

Amiot [24] confirmed the perturbations in the $v' = 0$ level by taking into account the $b^3\Sigma_g^-$ and the $B^1\Delta_g$ states. Recently, Tanabashi et al. [20,25] re-investigated the Swan system in detail by applying high-resolution Fourier transform spectroscopy for vibrational bands with $v' = 0 - 10$ and $v'' = 0 - 9$. Many line positions and assignments from earlier work [26], especially for $v' = 4, 5, 6$ had to be corrected. Perturbations were found for $v' = 0, 1, 2, 4, 6, 8, 9$ and 10. But the details of the perturbations could not be analyzed satisfactorily from the complex and overlapping band structure that were observed in the Fourier transform spectra. A recent study of the $d^3\Pi_g - c^3\Sigma_u^+$ system by Joester et al. [27] revealed perturbations in the $d^3\Pi_g, v' = 4$ level. The supersonically cooled radicals exhibiting only low J levels and, therefore, less congestion disclose perturbations that are in significant disagreement with the reported values from Tanabashi et al. [20,25].

In this work, we demonstrate the potential of two-color resonant four-wave mixing (TC-RFWM) in combination with a discharge source for the detailed characterization of the complex perturbations in the $d^3\Pi_g - a^3\Pi_u$ electronic system of C_2. In fact, we have shown recently on several transient species (C_3 [28], C_2 [29], HC_4S [29], HC_2S [30] and C_{2^-} [31]) that the excellent sensitivity of TC-RFWM is applicable to the low-density environment of a discharged free-jet. From the combination of the two experimental techniques new possibilities ensue for an advanced treatment of the perturbation problem. The corona discharge followed by the supersonic expansion produces molecules that are excited to high vibrational levels (2000–6000 K) but in each vibrational level a relatively low J population is present (50–100 K). The low rotational temperature spectra reducing the number of transitions in each band are ideal to determine accurate line positions. Furthermore, by taking advantage of the double-resonance capabilities of TC-RFWM, unambiguous assignments of perturbed transitions is often possible by intermediate level labeling. Thus, the combination of the discharge source with TC-RFWM spectroscopy results in a tremendous simplification of the complex one-color spectra obtained in microwave discharges by Fourier transform spectroscopy, CRD or LIF.

We outline the method by analyzing the perturbations between the $d^3\Pi_g, v' = 4$ and the $b^3\Sigma_g^-, v' = 16$ levels (Fig. 1). Several substantial perturbations are reported for the first time to the best of our knowledge. In addition, the observations yield numerous reassignments of perturbed transitions. Moreover, we show that for strong interactions between close-lying levels, perturber states are revealed and observed as extra lines which give further insight into the perturbation process.

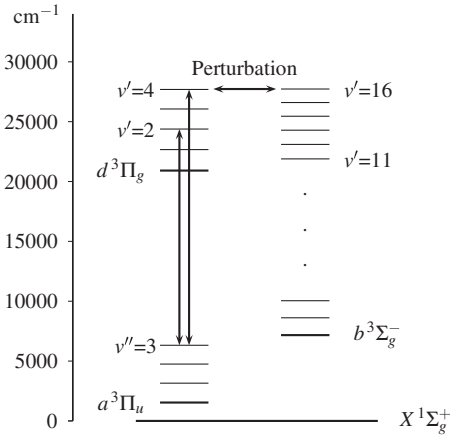

Fig. 1. Energy level diagram of the relevant vibronic states. Intermediate level labeling is performed in the (2,3) band of the $d^3\Pi_g - a^3\Pi_u$ transition. Perturbed levels from the interaction between $d^3\Pi_g, v' = 4$ and $b^3\Sigma_g^-, v' = 16$ are then observed from the common lower state in the (4,3) band. See text for details.

2. Experimental set-up

The molecular beam apparatus and the slit discharge assembly has been described previously in detail [28,29] and only a brief outline of the experiment is following. Radicals are generated by pulsing the precursor mixture of ≈0.5% acetylene in argon through a 30 × 1.0 mm slit-jet nozzle based on the design of Linnartz [32]. Pressures behind the valve are typically 5–7 atm. A high-voltage pulse of −800 to −1000 V is applied to the electrodes by using a precisely timed trigger pulse relative to the valve opening. In comparison with a cylindrical source, the two-dimensional slit-expansion increases the interaction volume of the four-wave mixing beams with the molecular beam and enhances the sensitivity of the method, In fact, experiments on the C_2 and HC_4S radicals resulted in high signal-to-noise ratios and a DFWM sensitivity among the highest achieved [29]. The molecular beam propagates into the vacuum chamber and interacts with the laser beams roughly 2 cm downstream from the discharged slit-jet exit. During operation a pressure of $\approx 10^{-2}$ Pa is maintained.

One or two separately pumped dye lasers (narrowscan, Radiant Dyes) are used for DFWM and TC-RFWM, respectively. The specified bandwidth of the laser systems is $\approx 0.04\ \text{cm}^{-1}$. Low pulse energies of ≈1 μJ/pulse are applied to avoid power broadening due to saturation of the transitions by applying variable attenuators (Newport, M-935-10). A combination of optical components establishes a forward BOXCARS [33] configuration [34]. The three input beams with wavevectors $\vec{k}_1, \vec{k}_2$ and $\vec{k}_3$ generate a signal beam wave vector $\vec{k}_4$. For the double-resonance TC-RFWM experiment, one of the three incident beams ($\vec{k}_2$) is replaced by a laser beam of different frequency (PROBE beam). The equal frequency input beams ($\vec{k}_1$ and $\vec{k}_2$) are commonly referred to as PUMP beams. The direction of the four-wave mixing signal beam is given by the phase-matching condition $\vec{k}_1 + \vec{k}_3 = \vec{k}_2 + \vec{k}_4$ and passes through several optical and spatial filters to remove interfering scattered light and unwanted fluorescence. Further reduction of stray light is achieved by a spatial filter consisting of a 30 mm focal length lens and 50 μm pinhole in front of the photomultiplier. Typically 20–30 pulses are averaged per scan step of the dye laser (5×10^{-4} nm/step) on the oscilloscope and transferred to a PC (labview) for further analysis.

3. Results and discussion

Fig. 2 depicts the wavelength region of the (4,3) band of the $d^3\Pi_g - a^3\Pi_u$ system. In addition transitions appear in this range that are due to other sequence bands such as (5,4) and (6,5). The bands are denoted by the standard nomenclature (v', v''). On the bottom, a simulation of the (4,3) band is shown inverted that has been computed by the pgopher program developed by Western [35] and using molecular constants from Tanabashi et al. [20,25]. As mentioned above, a global analysis of the rotational perturbations has not been performed and is neglected in the simulation. As a consequence, several predicted line positions are in disagreement with the measurement. For example, the $R_1(7)$ transition is computed at 21399.53 cm^{-1} but observed in the DFWM spectrum shifted by −0.57 cm^{-1} at 21398.96 cm^{-1}. The shift of $R_1(7)$ is marked by an arrow in the Fig. 2. But an unambiguous assignment of a pertubed rotational transition is often difficult or impossible in one-color spectra from methods such as DFWM, CRD or LIF. As a consequence, numerous assignments are in disagreement in the

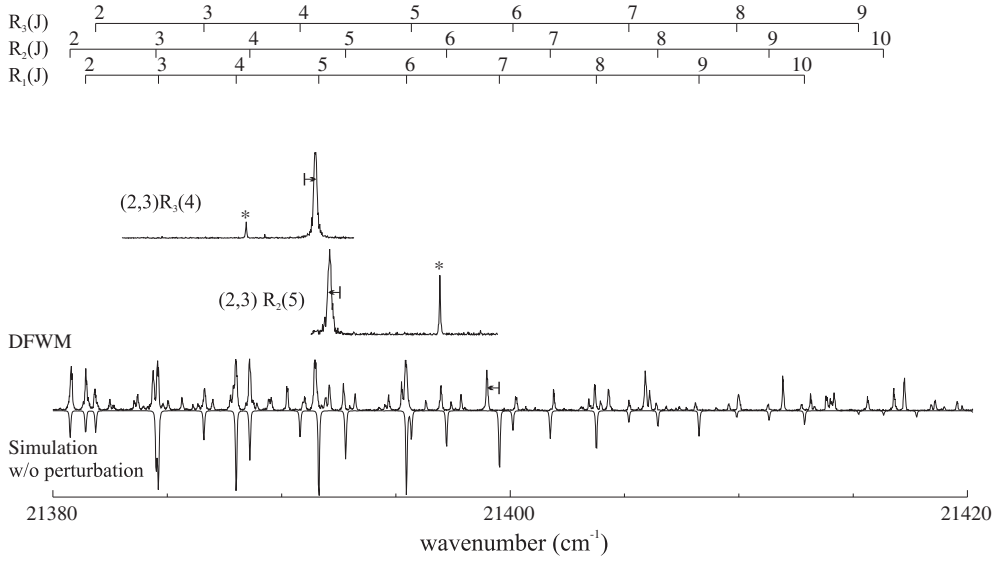

Fig. 2. DFWM and TC-RFWM in the wavelength region of the (4,3) sequence band of C_2. A comparison of the DFWM spectrum with a simulation of the (4,3) band neglecting perturbations (inverted trace) shows that several computed transitions are absent or shifted. By intermediate level labeling via the $R_2(5)$ and $R_3(4)$ transitions in the (2,3) band, unambiguous observation of $R_2(5)$ and $R_3(4)$ in the (4,3) band is achieved (two traces at the top). Both lines are shifted in respect to the simulation by ≈ 0.7 cm^{-1} but in opposite direction. In addition, extra lines appear due to the perturbing levels (marked with *). See text for details.

literature (*vide infra*). The use of two separate input frequencies for four-wave mixing proves advantageous in these situations, because a signal is obtained only when both frequencies interact with distinct molecular transitions simultaneously which share a common (lower) vibronic level. Two TC-RFWM spectra are shown in Fig. 2 and denoted by the fixed laser frequency used for intermediate level labeling. For the trace on the top, the $(2,3)R_3(4)$ rovibronic transition is utilized to label the $N''=5, J''=4, v''=3$ level in the $a^3\Pi_u$ electronic state. Subsequent scanning of the second frequency in the wavelength range of the (4,3) band yields transitions only that share this lower level. A dramatic simplification of the one-color (DFWM) spectrum is achieved. Two transitions are observed and assigned in a straightforward manner. The transition at 21391.47 cm^{-1} is due to the perturbed $(4,3)R_3(4)$ rotational transition that is shifted by +0.67 cm^{-1}. In addition, a second peak is present which is due to the $(16,3)^qR_{23}(4)$ transition. This transition is made visible by the interaction between the $N'=5, J'=5$ and $v'=16$ level of the perturber state $b^3\Sigma_g^-$ and the $N'=6, J'=5, v'=4$ level of the $d^3\Pi_g$ Swan state.

From first order perturbation theory [36], the secular determinant yields for the perturbed energy

$$E=\frac{1}{2}(E_1+E_2)\pm\frac{1}{2}\sqrt{4W_{12}^2+\Delta E^2} \quad (1)$$

where W_{12} is the matrix element of the perturbation and $\Delta E=E_1-E_2$ is the separation of the unperturbed levels. The shifts of the two levels $\delta E=E-E_1=E-E_2$ are equal in magnitude and are given by

$$\delta E=\pm\frac{1}{2}\left(\sqrt{4W_{12}^2+\Delta E^2}-\Delta E\right) \quad (2)$$

as illustrated in Fig. 3. Thus, the line shifts from the unperturbed levels and the distance from perturbed and perturbing transition are directly resulting from the magnitude of the perturbation matrix element W_{12}. Note however, that this perturbation theory applies for a simple two-level system only (for example $^1\Sigma\sim{}^1\Sigma$ interaction) and a more refined theory, taking into account effects such as spin-orbit interaction, has to be applied for the perturbation between $d^3\Pi_g$ and $b^3\Sigma_g^-$ (*vide infra*).

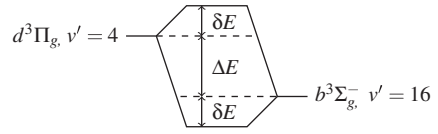

Fig. 3. The spectral separation observed between perturbed and perturbing transitions is given by $2\delta E+\Delta E$, where ΔE is the separation of the two levels in the absence of perturbation and δE is the displacement of the levels resulting from the perturbation.

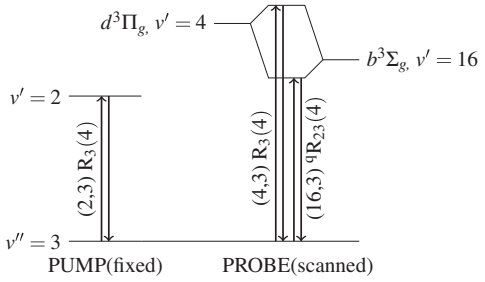

Fig. 4. Energy level schematic for the observation of perturbed/perturbing transitions by TC-RFWM. The perturbing (16,3) $^qR_{23}(4)$ and perturbed (4,3) $R_3(4)$ transitions are observed by labeling the ground state level $N''=5, J''=4$ with the PUMP laser fixed on the (2,3) $R_3(4)$ transition and scanning the PROBE in the (4,3) band. For clarity, the splitting of the perturbed levels is exaggerated. See text for details.

Fig. 4 depicts the TC-RFWM scheme that is applied to probe this perturbation. The PUMP laser wavelength is tuned to 18086.3 cm^{-1} exciting the $(2,3)R_3(4)$ transition while the PROBE laser is scanned in the (4,3) band disclosing the perturbation pair as shown in Fig. 2 (top trace). Similarly, a second TC-RFWM spectrum is reproduced in the figure which has been obtained by tuning the PUMP laser to the $(2,3)R_2(5)$ transition. Again a perturbed/perturbing pair is measured and assigned to $(4,3)R_2(5)$ $(d^3\Pi_g-a^3\Pi_u)$ and $(16,3)^qR_{12}(5)$ $(b^3\Sigma_g^--a^3\Pi_u)$ resp. The lines are shifted by −0.70 and +0.87 cm^{-1}, resp., from their unperturbed position. The results for $(4,3)R_3(4)$ and $(4,3)R_2(5)$ are in agree-

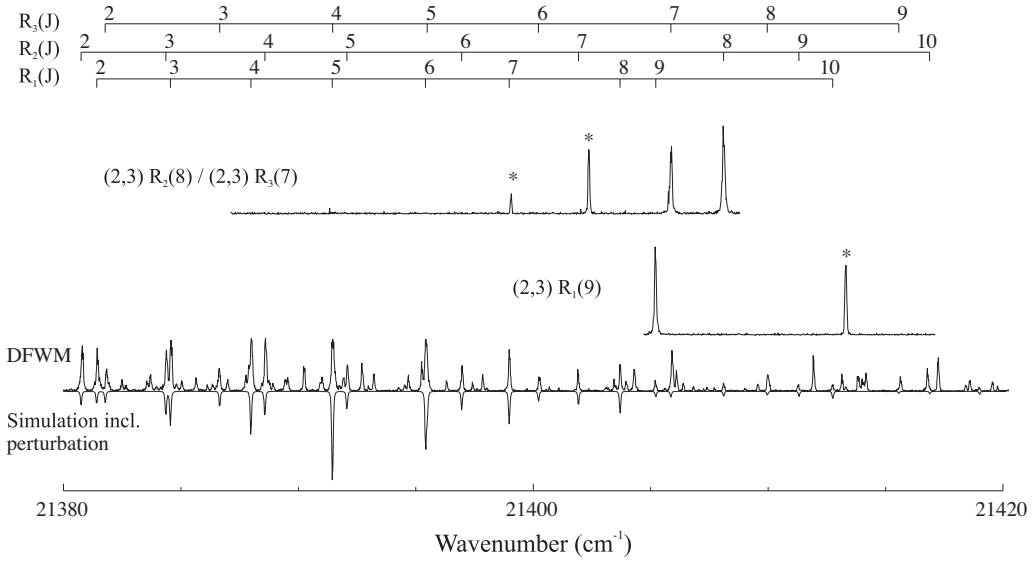

Fig. 5. DFWM and TC-RFWM in the wavelength region of the (4,3) sequence band of C_2. The DFWM spectrum is compared with a computation of the (4,3) band by taking into account perturbations by the $b^3\Sigma_g^-$, $v' = 16$ state (inverted). An overall good agreement is achieved by applying the molecular constants from the deperturbation analysis listed in Table 2. The predicted substantial shifts of $R_1(9)$ and $R_2(8)$(−3.06 and +1.65 cm^{-1}, resp.) are verified by TC-RFWM and shown in the two upper traces. Note that for the intermediate level labeling two transitions, $(2,3)R_2(8)$ and $(2,3)R_3(7)$, overlap and result in an additional perturbation pair ($(4,3)R_3(7)$ and $(16,3)R_3(7)$).

ment with line positions and assignments reported by Tanabashi [20,25] and more recently by Joester et al. [27].

As mentioned in the introduction, the $b^3\Sigma_g^-$ state has been found [21] to be responsible for perturbations in the $d^3\Pi_g$, $v' = 0, 1, 2$ states and suggested to perturb [23] the $J' = 5$ and 14 rotational levels of $d^3\Pi_g$, $v' = 4$. Unfortunately, accurate molecular constants for high lying vibrational levels of the $b^3\Sigma_g^-$ are not available. However, extrapolated values for $v' = 16$ are attainable by taking into account the Dunham coefficients reported by Amiot et al. [37] from the study of 13 bands between (0,0) and (6,3) in the Ballik–Ramsay system ($b^3\Sigma_g^- - a^3\Pi_u$). The results of the extrapolation are listed in Table 2. An inspection of the molecular constants for the $b^3\Sigma_g^-$, $v' = 16$ predicts a crossing with the $d^3\Pi_g$, $v' = 4$ at low J values. Thus, a perturbation model is assumed that takes into account a $^3\Pi_g \sim {}^3\Sigma_g^-$ interaction.

It is possible to obtain an initial guess of the perturbation parameters by fitting the four assigned levels to a model that takes into account spin-orbit interaction and L-uncoupling effects [38] between $d^3\Pi_g$, $v' = 4$ and $b^3\Sigma_g^-$, $v' = 16$. Apart from the two perturbation parameters, the vibrational origin T and rotational constant B of the perturber state is included as fitting parameters. Owing to the low J numbers measured in this study, the centrifugal distortion constant, D, of the perturbing state is fixed at the extrapolated value of Amiot et al. [37]. Interestingly, the initial procedure has resulted in the prediction of several new perturbations that were not reported in the literature. The TC-RFWM spectra in Fig. 5 shows the validation of two predicted perturbations for $(4,3)R_1(9)$ and $(4,3)R_2(8)$. In fact, by fixing the PUMP laser on $(2,3)R_1(9)$ a large shift of −3.06 cm^{-1} for the $(4,3)R_1(9)$ transition is observed (second trace from top). In addition, the spectrum shows an intense perturber transition at 21413.30 cm^{-1} which is assigned as $(16,3)R_1(9)$. This line exhibits a shift of +2.95 cm^{-1}.

The top trace in Fig. 5 shows a remarkable TC-RFWM scan that is observed by tuning the PUMP laser to the position of $(2,3)R_2(8)$. This transition at 18103.1 cm^{-1} coincides with $(2,3)R_3(7)$. Therefore, both rotational levels, $N'' = 8, J'' = 8, v'' = 3$ and $N'' = 8$, $J'' = 7, v'' = 3$ are labeled. The resulting TC-RFWM scan of the PROBE laser in the (4,3) band reveals two perturbation pairs, since both upper rotational levels of the $d^3\Pi_g$, $v' = 4$ interact with levels in $b^3\Sigma_g^-$, $v' = 16$: $(4,3)R_2(8)$ is shifted by +1.65 cm^{-1} and $(4,3)R_3(7)$ by +0.67 cm^{-1}. Also, both perturber states are observed with significant intensities and marked with asterisks in the spectrum.

Table 1 lists 23 perturbed transitions and 12 extra lines observed by TC-RFWM and assigned unambiguously by intermediate level labeling. Note that in many cases the perturbations are measured in the P and R branch thus impeding ambiguities due to perturbations in the lower $a^3\Pi_u$, $v'' = 3$ state. For example, both the $R_2(5)$ and $P_2(7)$ transitions yield the shift of the upper $F_2, J' = 6$ level (−0.70 cm^{-1}). The intermediate level state in $v'' = 3$ on the other hand is different ($F_2, J'' = 5$ and $F_2, J'' = 7$). In addition, literature data from Tanabashi et al. [20,25], Joester et al. [27] and Phillips and Davis[26] are included in Table 1 where available. Numerous perturbations in the (4,3) band are reported for the first time to the best of our knowledge. In particular, the significantly perturbed $R_1(9)$ and $P_1(11)$ and to a less extend the $R_2(8)$ and $P_2(10)$ lines have not been observed before. Important disagreement with Refs. [20,25] is found for $R_3(3)$, $P_3(5)$, $R_3(5)$ and $P_3(7)$. These findings have been observed also in the recent study of the (4,1) band in the $d^3\Pi_g - c^3\Sigma_u^+$ system [27]. In our work, more inconsistencies are found for the $R_1(12)$ and $P_1(14)$ transitions. However, the 13 remaining transitions are in good agreement with our results. On the other hand, most of the values of Phillips and Davis [26] are in disagreement with our measurements. For the 12 extra lines no literature data is available for comparison.

It is important to mention that the reduction of the perturbations is very difficult to achieve without the determination of accurate shifts and the measurements of extra lines. In this work, the simplification of the complex spectra by intermediate level labeling results in the unambiguous determination of the line positions of perturbed transitions *and* allows the observation of the extra lines. Predicted line shifts and the positions of numerous extra lines are measured in a straightforward manner to validate the perturbation model. Molecular constants including perturbation parameters are obtained by performing a least-squares optimization procedure to all listed transitions using pgopher [35] and shown in the fourth column of Table 2. The fit is significantly improved by inclusion of the spin-spin coupling parameter, λ. For comparison, a fit without taking into account extra lines is shown in the third column of the table. The root mean square value for

Table 1
Observed positions and shifts of perturbed transitions due to the interaction of the Swan $d^3\Pi_g, v' = 4$ state and $b^3\Sigma_g^-, v' = 16$ measured by TC-RFWM. The last column lists the residuals to a synthetic spectrum taking into account optimized perturbation parameters listed in Table 2. The root mean square of the residuals is 0.02 cm^{-1}.

Upper electronic state	Transition	Observed	Perturbation				Residuals
			This work	Ref. [27][a]	Ref. [20,25]	Ref. [26]	
$d^3\Pi_g, v' = 4$	$R_1(7)$	21398.96	−0.57	−0.57	−0.52	−0.97	−0.02
	$R_1(9)$	21405.20	−3.06	–	–	−0.93	−0.02
	$P_1(11)$	21344.55	−3.05	–	–	−0.74	−0.01
	$R_1(12)$	21422.20	−0.53	–	1.28	−0.57	−0.02
	$P_1(14)$	21343.05	−0.52	–	1.17	−0.53	−0.01
	$P_1(15)$	21343.33	0.71	–	0.73	0.05	−0.04
	$R_2(5)$	21392.10	−0.70	−0.76	−0.69	−0.99	0.03
	$P_2(7)$	21351.70	−0.70	−0.76	−0.67	−0.68	0.03
	$R_2(8)$	21408.10	1.65	–	–	−0.28	0.00
	$P_2(8)$	21350.10	−0.24	–	−0.20	−0.71	0.02
	$P_2(9)$	21348.79	0.17	–	0.20	−0.60	0.00
	$P_2(10)$	21348.55	1.65	–	–	−0.23	0.00
	$P_2(11)$	21345.48	−0.03	–	−0.02	−0.69	−0.03
	$R_2(12)$	21427.19	0.37	–	0.42	−0.58	−0.04
	$R_3(3)$	21386.64	0.04	−0.03	−1.54	−1.48	−0.01
	$R_3(4)$	21391.47	0.67	0.63	0.71	−1.04	0.00
	$R_3(5)$	21395.49	−0.19	−0.30	1.31	−1.13	0.00
	$P_3(5)$	21354.06	0.04	−0.03	−1.62	−0.99	−0.01
	$P_3(6)$	21352.38	0.72	0.63	0.73	−1.24	0.05
	$R_3(7)$	21405.87	0.67	–	0.71	−0.87	0.01
	$P_3(7)$	21349.58	−0.21	−0.30	1.59	−0.85	−0.02
	$P_3(8)$	21347.97	0.15	–	0.15	−0.70	0.04
	$P_3(10)$	21344.78	0.08	–	0.04	−0.51	0.02
$b^3\Sigma_g^-, v' = 16$	$R_1(7)$	21417.38	0.32				−0.01
	$R_1(9)$	21413.30	2.95				0.00
	$P_1(11)$	21352.65	2.95				0.00
	$^sR_{21}(12)$	21427.86	0.07				0.01
	$^qP_{21}(14)$	21348.69	0.06				0.00
	$^qR_{12}(5)$	21396.93	0.87				−0.01
	$^oP_{12}(7)$	21356.52	0.86				−0.01
	$R_2(8)$	21402.37	−1.64				−0.01
	$P_2(10)$	21342.81	−1.64				−0.01
	$^qR_{23}(4)$	21388.45	−0.59				0.00
	$^oP_{23}(6)$	21349.30	−0.59				0.00
	$R_3(7)$	21399.06	−0.59				0.03

[a] Averaged values of transitions from the (4,1) band of the $d^3\Pi_g - c^3\Sigma_u^+$ system.

Table 2
Optimized molecular constants for the perturbing $b^3\Sigma_g^-, v = 16$ state and parameters resulting from the interaction with the $d^3\Pi_g, v' = 4$ state. All values are in cm^{-1}. The origin, T, is relative to the $a^3\Pi_u, v'' = 0$ level. Numbers in parenthesis are one standard deviation.

State	Parameter	Optimized w/o extra lines	Optimized value	Extrapolated[a]
$b^3\Sigma_g^-, v' = 16$	T	26192.081(72)	26191.865(14)	26187.074
	B	1.22508(98)	1.22858(15)	1.22824
	$D \times 10^6$	6.4351[b]	6.4351[b]	6.4351[b]
	λ	0.32(11)	0.172(18)	0.155
$\langle d^3\Pi_g, v' = 4 \vert \mathbf{H}_{SO} \vert b^3\Sigma_g^-, v' = 16\rangle$		−0.6120(167)	−0.6401(86)	
$\langle d^3\Pi_g, v' = 4 \vert B\mathbf{L}_+ \vert b^3\Sigma_g^-, v' = 16\rangle$		0.2459(13)	0.24737(61)	

[a] Ref. [37].
[b] Fixed at the extrapolated value.

both reductions are ≈ 0.02 cm^{-1}. However, the inclusion of the extra lines yields significantly modified B and λ parameters. The improved agreement with the extrapolated values from Ref. [37] cleary support the assignment of the perturber state and emphasizes the importance of extra line measurements for the determination of accurate molecular constants of the perturbing state and the perturbation parameters.

4. Conclusion

We have shown that the application of double-resonant four-wave mixing is advantageous for the unambiguous assignment of perturbed and perturbing transitions by intermediate level labeling. The potential of the method is outlined by analyzing the interaction between the upper Swan level $d^3\Pi_g, v' = 4$ and the $b^3\Sigma_g^-, v' = 16$ state of C_2. Several new perturbations are observed, including the strongly perturbed transitions $R_1(9)$ and $P_1(11)$ that are shifted by more than 3 cm^{-1} in respect to their unperturbed positions. Spin-orbit and L-uncoupling parameters are used to rationalize the perturbation and deperturbed molecular constants for the $b^3\Sigma_g^-, v' = 16$ are obtained by applying a least-squares fitting to the observed transitions. Further work is performed to characterize in detail perturbations of other vibrational levels of the $d^3\Pi_g$ state, a task that is more involved owing

to multiple electronic states that interact simultaneously with the Swan levels. In fact, the higher J-levels of the $d^3\Pi_g, v' = 4$ state are further perturbed by the $B^1\Delta_g, v' = 12$ level. Its effect on the investigated perturbation is relatively small and not yet included in the analysis.

Acknowledgments

This work is supported by the Swiss Federal Office of Energy (100708) and the Swiss National Science Foundation (200020-124542/1).

References

[1] G.P. Smith, C. Park, J. Schneiderman, J. Luque, Combustion and Flame 141 (2005) 66–77.
[2] X. Mercier, E. Therssen, J. Pauwels, P. Desgroux, Proceedings of the Combustion Institute 30 (2005) 1655–1663.
[3] C. Kaminski, P. Ewart, Applied Physics B: Lasers and Optics 61 (1995) 585–592.
[4] C.F. Kaminski, I.G. Hughes, P. Ewart, The Journal of Chemical Physics 106 (1997) 5324–5332.
[5] K. Nyholm, M. Kaivola, C. Aminoff, Optics Communications 107 (1994) 406–410.
[6] J.B. Wills, J.A. Smith, W.E. Boxford, J.M.F. Elks, M.N.R. Ashfold, A.J. Orr-Ewing, Journal of Applied Physics 92 (2002) 4213–4222.
[7] A. Staicu, R.L. Stolk, J.J. ter Meulen, Journal of Applied Physics 91 (2002) 969–974.
[8] A. Goldman, S. Cheskis, Applied Physics B: Lasers and Optics 92 (2008) 281–286.
[9] J. Walewski, M. Rupinski, H. Bladh, Z. Li, P. Bengtsson, M. Alden, Applied Physics B: Lasers and Optics 77 (2003) 447–454.
[10] P.E. Bengtsson, M. Alden, Applied Physics B: Lasers and Optics 60 (1995) 51–59.
[11] J.J. Camacho, L. Diaz, M. Santos, D. Reyman, J.M.L. Poyato, Journal of Physics D: Applied Physics 41 (2008) 105201.
[12] S. Abdelli-Messaci, T. Kerdja, A. Bendib, S. Malek, Journal of Physics D: Applied Physics 35 (2002) 2772–2778.
[13] S.S. Harilal, R.C. Issac, C.V. Bindhu, V.P.N. Nampoori, C.P.G. Vallabhan, Journal of Applied Physics 81 (1997) 3637–3643.
[14] R. Issac, C. Bindhu, V. Nampoori, C. Vallabhan, S. Harilal, Journal of Physics D: Applied Physics 30 (1997) 1703–1709.
[15] J.E.M. Goldsmith, D.T.B. Kearsley, Applied Physics B: Lasers and Optics 50 (1990) 371–379.
[16] P. Bengtsson, M. Alden, Combustion and Flame 80 (1990) 322–328.
[17] R.I. Kaiser, Chemical Reviews 102 (2002) 1309–1358.
[18] P. Rousselot, S.M. Hill, M.H. Burger, D.A. Brain, C. Laffont, G. Moreels, Icarus 146 (2000) 263–269.
[19] G.M. Lloyd, P. Ewart, The Journal of Chemical Physics 110 (1999) 385–392.
[20] A. Tanabashi, T. Hirao, T. Amano, P.F. Bernath, The Astrophysical Journal Supplement Series 169 (2007) 472–484.
[21] J. Callomon, A.C. Gilby, Canadian Journal of Physics 41 (1963) 995–1004.
[22] M. Douay, R. Nietmann, P. Bernath, Journal of Molecular Spectroscopy 131 (1988) 261–271.
[23] J.G. Phillips, Journal of Molecular Spectroscopy 28 (1968) 233–242.
[24] C. Amiot, Astrophysical Journal Supplement Series 52 (1983) 329–340.
[25] A. Tanabashi, T. Hirao, T. Amano, P.F. Bernath, The Astrophysical Journal Supplement Series 170 (2007) 261.
[26] J.G. Phillips, S.P. Davis, in: The Swan System of the C2 Molecule and the Spectrum of the HgH Molecule, Cambridge University Press, London, UK, 1968, pp. 1–12.
[27] J.A. Joester, M. Nakajima, N.J. Reilly, D.L. Kokkin, K. Nauta, S.H. Kable, T.W. Schmidt, The Journal of Chemical Physics 127 (2007) 214303–214306.
[28] M. Tulej, M. Meisinger, G. Knopp, A.M. Walser, T. Gerber, P.P. Radi, Journal of Raman Spectroscopy 38 (2007) 1022–1031.
[29] F.J. Mazzotti, E. Achkasova, R. Chauhan, M. Tulej, P.P. Radi, J.P. Maier, Physical Chemistry Chemical Physics 10 (2008) 136–141.
[30] J.P. Maier, R. Chauhan, F.J. Mazzotti, R. Raghunandan, M. Tulej, P.P. Radi, Journal of Physical Chemistry (2009).
[31] M. Tulej, T. Gerber, G. Knopp, P.P. Radi, Journal of Raman Spectroscopy, in press. doi:10.1002/jrs.2638.
[32] H. Linnartz, Physica Scripta 69 (2004) C37–C40.
[33] Y. Prior, Applied Optics 19 (1980). 1741_1–1743.
[34] P.P. Radi, H.M. Frey, B. Mischler, A.P. Tzannis, P. Beaud, T. Gerber, Chemical Physics Letters 265 (1997) 271–276.
[35] C.M. Western, PGOPHER, A Program for Simulating Rotational Structure, 2009.
[36] G. Herzberg, Spectra of Diatomic Molecules, second ed., Van Nostrand Reinhold Company, New York, 1950.
[37] C. Amiot, J. Chauville, J.P. Maillard, Journal of Molecular Spectroscopy 75 (1979) 19–40.
[38] H. Lefebvre-Brion, R.W. Field, The Spectra and Dynamics of Diatomic Molecules, Elsevier Academic Press, Amsterdam, 2004 (Revised and Enlarged Edition).